

Research Article

Purification of Urban Sewage River Using a Biological Aerated Filter with Sponge Iron and Ceramsite Mixed Fillers

Yi Wu ¹, Jun Dai ¹, Qiong Wan ¹, Guobin Tian ¹ and Dongyang Wei ²

¹School of Architecture and Civil Engineering, Xi'an University of Science and Technology, Xi'an, Shaanxi 710054, China

²South China Institute of Environmental Sciences, Guangzhou, Guangdong 510655, China

Correspondence should be addressed to Yi Wu; 19104053009@stu.xust.edu.cn

Received 31 August 2020; Revised 12 December 2020; Accepted 17 December 2020; Published 28 December 2020

Academic Editor: Valeria Vignali

Copyright © 2020 Yi Wu et al. This is an open access article distributed under the Creative Commons Attribution License, which permits unrestricted use, distribution, and reproduction in any medium, provided the original work is properly cited.

Filler plays an important role in biological sewage treatment technology. In the purification of urban sewage river, the single sponge iron filler is easy to harden. The combination of sponge iron and ceramsite can hinder the hardening and improve the removal efficiency. In this paper, scanning electron microscopy (SEM) and X-ray diffraction (XRD) were used to characterize the fillers. The removal efficiency experiments were carried out through the self-designed biological aerated filter (BAF) reactor with sponge iron and ceramsite mixed fillers, and the microorganisms attached to the surface of the biological fillers were qualitatively and quantitatively identified through 16S rDNA. The results indicate that the presence of Fe_3O_4 , Fe_2O_3 , Fe_3C , and Fe_2CO_3 in sponge iron determines that sponge iron has strong reducibility and provides electrons for efficient denitrification. $\text{NaAlSi}_3\text{O}_8$ in ceramsite filler plays a significant role in phosphorus adsorption. In #3, #4, and #5 reactors (the mass ratios of sponge iron and ceramsite were 1 : 1, 3 : 1, and 1 : 3, resp.), the removal efficiencies of mixed fillers are good on chemical oxygen demand (COD), total phosphorus (TP), and nitrogen (N), and the more the ceramsite fillers in the reactors are, the higher the microbial abundance and diversity are. The mixture of sponge iron and ceramsite can be used to purify urban sewage river. A scientific basis to purify the polluted water body of urban rivers in situ is thus provided.

1. Introduction

Inland urban rivers are indispensable to the economic development and daily activities of urban populations. Specifically, because many of these rivers are used as water sources [1, 2], they affect the quality of daily life of nearby urban populations. Thus, economically efficient green technology purposed for river purification (particularly, in situ river purification) is becoming increasingly popular [3, 4].

According to the current research, in the system composed of biofiltration materials, aquatic plants, and their attached microorganisms, the absorption and removal of pollutants in polluted water by plants account for 10%–15%, while the removal of organic pollutants by substrate is also mainly manifested in the adsorption of total phosphorus (TP), and it is microorganisms that play a major role in the removal and purification [5]. However, in cold regions such

as Northwestern China, plant death is inevitable, and the amount of microbes is reduced. Therefore, urban sewage river cannot be effectively purified. Zeolite and ceramsite were used to purify the secondary effluent from the wastewater plant [6], and the purification performance and manufacturing technology of zeolite and ceramsite fillers were further analyzed and studied. It is found that zeolite and ceramsite exhibited good purification ability and a high anti-impact load capacity. For a gas-water volume ratio of 3 : 1, the hydraulic load was $1 \text{ m}^3 \text{ m}^{-2} \text{ h}^{-1}$. Under the conditions of temperatures ranging between 20°C to 25°C and 15°C to 19°C, the chemical oxygen demand (COD) removal efficiencies of zeolite biological aerated filter (BAF) and ceramsite BAF were 12.67% and 21.93%, and the $\text{NH}_3\text{-N}$ removal efficiencies were 96.64% and 97.79%, respectively. The secondary effluent of wastewater for making soy sauce was treated by ceramsite and sponge iron mixed fillers [7]. The results show that when the filler layer height was 100 cm,

the water color and COD removal efficiencies reached 64.4% and 58.4%, respectively. Alternatively, biofilm treatment technology was purposed to produce unique and effective immobilized microbial carrier materials [8, 9]. The roughness and charge at the surface of the carrier materials are critical factors that affect the immobilization rate, and the carrier materials also have the advantages of high activity, high stability, and high resistance to microbial decomposition [10]. However, sponge iron has the advantages of a large specific surface area, high porosity, high surface energy, and strong reducibility [11]. In consideration of these advantages, Through the study on the reduction of nitrate and facilitating the removal of phosphorus in domestic sewage with sponge iron filler [12, 13], it can be known that the small size of the sponge iron particles and consequential increase in the solid-liquid ratio facilitated nitrate reduction. Additionally, the combined action of zero-valent iron and microorganisms effectively removed phosphorus. However, there is a serious hardening phenomenon in the use of sponge iron. Sponge iron hardening will reduce the specific surface area and porosity of the fillers, thus reducing the treatment effect [14, 15]. Therefore, the hardening problem of sponge iron needs to be studied and solved. The ceramsite filler has become one of the main processes for biological pretreatment of micropolluted water sources due to its low cost and easy availability, good biocompatibility, rough surface, developed pores, and so on.

Sponge iron and ceramsite fillers were selected for mixing to give full play to the advantages of fillers to improve the removal efficiencies, and the purification effect of the mixed fillers was studied. This work could provide a scientific basis for the purification of urban sewage river.

2. Materials and Methods

2.1. Experimental Materials and Device. Industrial sponge iron and ordinary clay ceramsite were used as fillers in this experiment. Sponge iron filler was purchased from the experimental filter material jointly developed by Beijing Jinke Composite Material Co., Ltd. and Wuhan Water Conservancy University, China. The ceramsite filler was purchased from the Gongyi Huixin Water Purification Company of China. The fillers were screened, washed with deionized water, and dried in an oven at 50°C for later use. The main characteristics of sponge iron and ceramsite are listed in Tables 1 and 2.

The experimental water was from a river in Lintong District, Xi'an, China. As a flood discharge river, it is usually discharged into domestic sewage and is the receiving water body of sewage treatment plant.

The device was made using 8 mm thick organic glass (Figure 1). The test water was injected in the inlet on the left side of the reactor using a peristaltic pump, fully treated in the reaction zone consisting of sponge iron and ceramsite fillers, and then discharged in the outlet. A partition was installed in the device to control the hydraulic residence time. Additionally, the bottom of the reactor was equipped with aeration with an adjustable flow rate according to the experiment design. The intermittent inlet and outlet water

were used in all the tests. The length, width, and height of the device were 40 cm, 12 cm, and 60 cm, respectively, and the effective volume was 28 L. There was a 4 cm high water collecting space at the bottom. The upper part of the water collecting space was filled with 25 cm thick mixed fillers, and the designed water depth was 55 cm.

2.2. Experiment Grouping and Test Method. The experiment was divided into six groups, that is, Ctrl, #1, #2, #3, #4, and #5. Ctrl was a blank control test without filler and was conducted under the same conditions and environment as the other five groups. #1 was pure sponge iron filler (16.5 kg of sponge iron). #2 was pure ceramsite filler (10.95 kg of ceramsite). #3 was mixed fillers with sponge iron and ceramsite mass ratio of 1:1 (6.06 kg of sponge iron and 6.06 kg of ceramsite). #4 was mixed fillers with sponge iron and ceramsite mass ratio of 3:1 (10.8 kg of sponge iron and 3.6 kg of ceramsite). #5 was mixed fillers with sponge iron and ceramsite mass ratio of 1:3 (3 kg of sponge iron and 9 kg of ceramsite).

After water change at 2 pm every day for 2 consecutive months in each group, the operation of the device was basically stable, and after that, samples were taken before water change every other day. At the same time, direct sampling from the sewage river was used as a reference to raw water. Each sample was tested in three groups and averaged. A peristaltic pump was used to inject 8 L raw water into each group each time, and the water exchange ratio of #1–#5 was approximately 1:2, and hydraulic retention time (HRT) was approximately 48 h. During the experiment, the average amount of dissolved oxygen (DO) for the six groups remained within the range of 3.22 mg/L–3.35 mg/L, the water temperature was 6°C–23°C, and the pH was 5.5–8.

Samples of fresh sponge iron and fresh ceramicite were taken before the experiment and samples of biological sponge iron and biological ceramicite were taken after the experiment for SEM analysis. The samples were dried and sprayed with gold film and then placed on the loading table, pressed lightly, and fixed with conductive adhesive. SEM uses focused electron beam scanning imaging on the sample surface point by point. From the electron microscope images under different magnification, the pore and three-dimensional morphological characteristics of the surface microstructure of sponge iron and ceramsite fillers can be intuitively seen. Samples of biological sponge iron and biological ceramicite were taken for 16rDNA analysis after the experiment.

The indexes and methods [16, 17] that were adopted for testing are listed in Table 3. The SEM was obtained from the Analysis and Test Center of the South China University of Technology, and 16S rDNA analysis was accomplished by Meg Gene Technology Co., Ltd.

The SDS method was used for DNA extraction, 16S V4 primers (515F and 806R) were used to identify bacterial diversity, 18S V4 primers (528F and 706R) were used to identify eukaryotic microbial diversity, and ITS1 primers (ITS5-1737F and ITS2-2043R) were used to identify fungal diversity. In addition, the amplification region also included

TABLE 1: Main characteristics of sponge iron filler.

| Fe content (%) | Sludge content (%) | Bulk density (T/m^3) | Particle diameter (mm) |
|----------------|--------------------|--------------------------|------------------------|
| ≥ 90 | ≤ 2 | 1.4–1.8 | 1–4.5 |

TABLE 2: Main characteristics of ceramsite filler.

| Porosity (%) | Particle diameter (mm) | Bulk density (g/cm^3) | Specific surface area (cm^2/g) |
|--------------|------------------------|---------------------------|-------------------------------------|
| 55–58 | 0.5–5 | 0.7–1.2 | 2×10^4 – 1.5×10^5 |

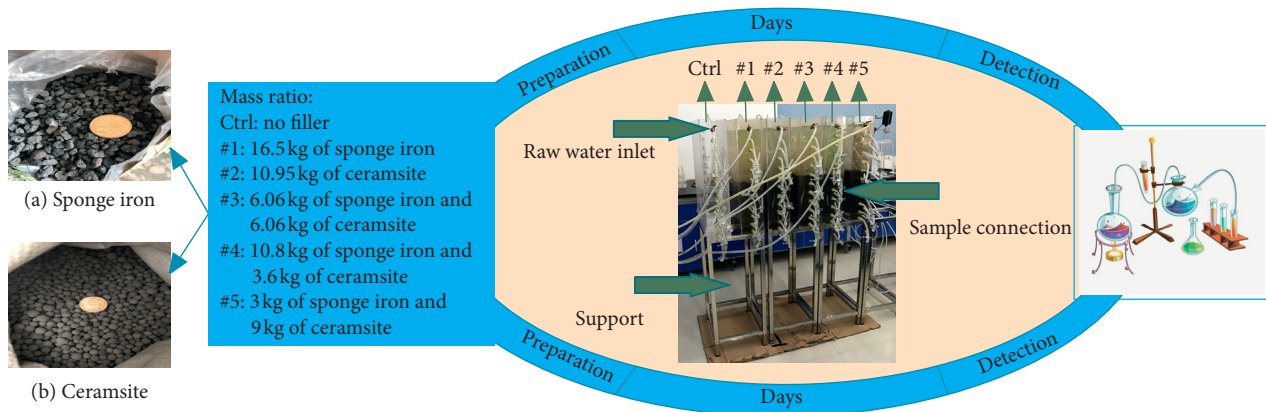


FIGURE 1: Simplified model of the mixed fillers test device.

TABLE 3: Test indexes and methods.

| Indexes | Methods | According to | Remark |
|-------------------------|---|-----------------|----------------|
| COD | Potassium dichromate method | CNS11914-89 | Self-detection |
| NH_3-N | Nessler's reagent colorimetric method | HJ535-2009 | Self-detection |
| TP | Ammonium molybdate spectrophotometric method | CNS11893-89 | Self-detection |
| TN | Alkaline potassium persulfate digestion ultraviolet spectrophotometry | HJ636-2012 | Self-detection |
| Filler characterization | SEM | Hitachi S-3700N | Submission |
| Microorganism | 16S rDNA | — | Submission |

16S V3-V4 /16S V4-V5, archaea 16S V4-V5, 18S V5, and ITS2, and primers corresponding to functional genes. The total number of sequences and operational taxonomic units (OTUs) of biofilm samples of each group are shown in Table 4 and the OTU classification information is shown in Table 5.

3. Results and Discussion

3.1. Characterization of Fresh Sponge Iron and Ceramsite

3.1.1. SEM Characterization. According to relevant literature [18, 19], the optimum microbial growth condition of the fillers was $1 \mu m$ – $3 \mu m$ micropores. Therefore, in this study, a $1 \mu m$ – $2 \mu m$ magnification was applied to obtain SEM images of the fillers. Figure 2(a) shows a magnified electron microscope image of sponge iron surface following high-temperature calcination, cooling, and screening. The surface of the sponge iron has the loose, porous, and uneven three-dimensional structure. The rough three-dimensional surface greatly increases the specific surface area, which is not only

TABLE 4: Total number of sequences and OTUs of biofilm samples of each group.

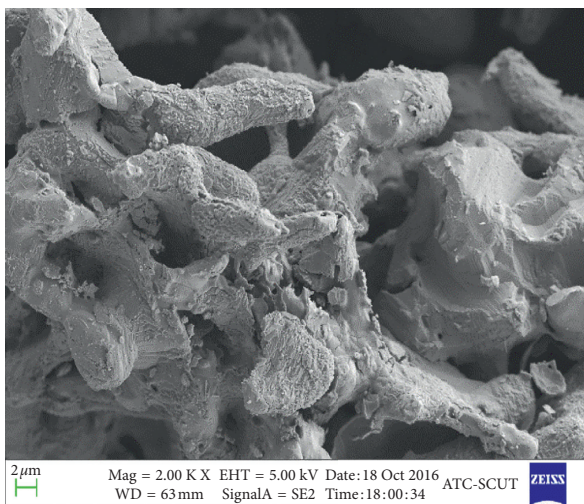
| Sample | Ctrl | #1 | #2 | #3 | #4 | #5 |
|-------------|-------|-------|-------|-------|-------|-------|
| No. of seqs | 22462 | 19751 | 15149 | 29283 | 23026 | 19133 |
| No. of OTUs | 842 | 622 | 762 | 359 | 474 | 745 |

conductive to the adsorption of pollutants in water, but also conducive to the growth and reproduction of microorganisms. Therefore, sponge iron is ideal for bioreactor.

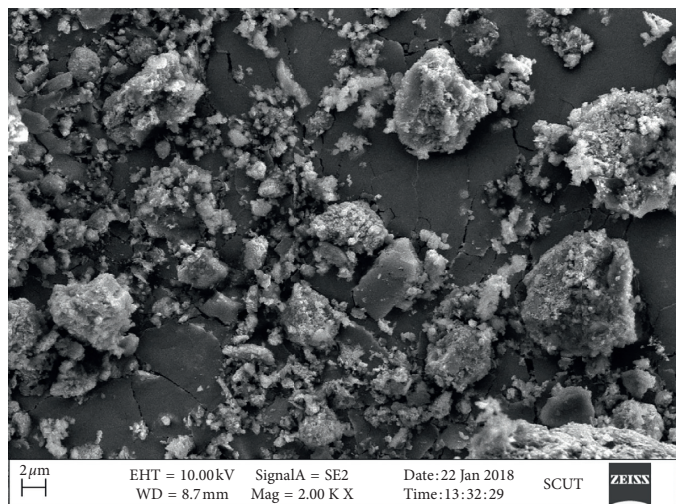
The surface of the fresh ceramsite has many rough convex surfaces with different sizes (typically $8 \mu m$ or less) and different shapes shown in Figure 2(b), and the specific surface area is large. The porous structure of both sponge iron and ceramsite is suitable for the growth of microorganisms and they are ideal fillers for bioreactors. The developed void structure and rough surface of sponge iron and ceramsite mixed fillers are not only conducive to the mass growth and reproduction of microorganisms, with high adsorption performance and adsorption capacity, but also

TABLE 5: The OTU classification information.

| OTU | Ctrl | #1 | #2 | #3 | #4 | #5 | Taxonomy |
|--------|------|-------|-------|---------|-------|------|--|
| OTU1 | 79.0 | 211.0 | 54.0 | 12438.0 | 124.0 | 75.0 | k_Bacteria p_Firmicutes c_Bacilli o_Bacillales f_Exiguobacteraceae g_ s_ k_Bacteria p_Proteobacteria c_Gammaproteobacteria o_Pseudomonadales f_Pseudomonadaceae g_Pseudomonas k_Bacteria p_Proteobacteria c_Gammaproteobacteria o_Thiotrichales f_Thiotrichaceae g_Thiothrix s_ |
| OTU10 | 35.0 | 49.0 | 35.0 | 1413.0 | 35.0 | 28.0 | |
| OTU100 | 0.0 | 3.0 | 172.0 | 1.0 | 0.0 | 82.0 | |



(a)



(b)

FIGURE 2: Electron microscope images, (a) fresh sponge iron and (b) fresh ceramsite.

can evenly distribute the air-water flow, reduce the scouring of air-water flow to the biofilm, stabilize the growth of biofilm, and enhance the biological treatment effect [20, 21].

3.1.2. XRD Characterization. In order to obtain the morphology of Fe in fresh sponge iron, the XRD analysis shown in Figure 3(a) was carried out. It is concluded that Fe_3O_4 , Fe_2O_3 , Fe_3C , and Fe_2CO_3 coexist in the sample with Fe. The presence of these substances determines that sponge iron has strong reducibility and provides reducing electrons for efficient denitrification. XRD indicates that the phases of sponge iron are dominated by Fe, accompanied by Fe_2O_3 , Fe_3O_4 , Fe_2CO_3 , and Fe_3C . Then, the specific content of each

component in the phase can be further obtained through quantitative analysis and calculation.

The ceramsite filler phases include $\text{LiGaSi}_2\text{O}_6$, $\text{NaAlSi}_3\text{O}_8$, $\text{Cu}(\text{HSeO}_3)_2$, LiNbMoO_6 , $\text{SC}(\text{N}_2\text{H}_3)_2$, Na_4H_4 , and $\text{SH}_6\text{N}_4\text{S}$ shown in Figure 3(b). The adsorption capacity of the ceramsite to phosphorus and ammonia nitrogen is not only related to the surface void structure of the filler but also related to the content of aluminum, iron, and their corresponding oxides [22]. Therefore, $\text{NaAlSi}_3\text{O}_8$ plays a significant role in the adsorption of ceramsite filler. The results show that the content of aluminum and Fe has a significant effect on the TP removal. Under the same environmental conditions, the lower the content of aluminum and Fe, the worse the adsorption of TP.

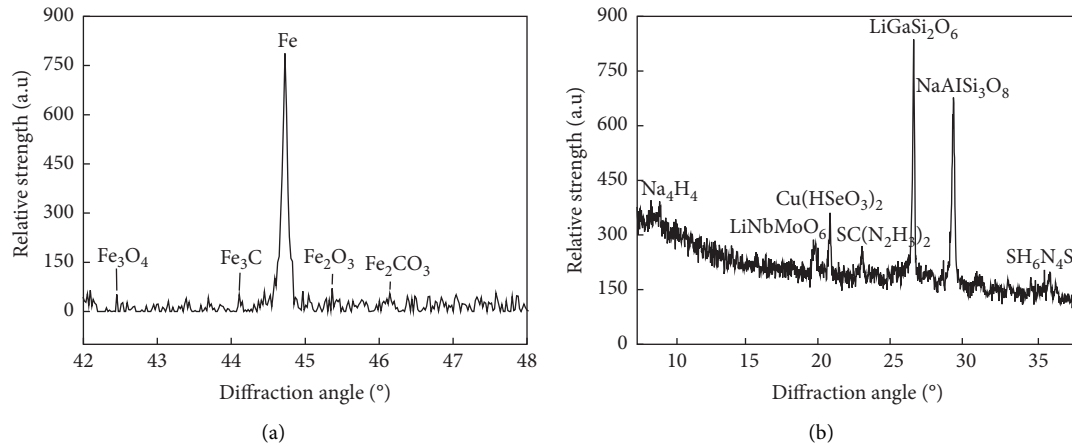


FIGURE 3: XRD graphs, (a) fresh sponge iron and (b) fresh ceramsite.

3.2. Characterization of Biological Sponge Iron and Ceramsite.

A biofilm was formed on the filler surface after the device had been operated for a period of time. After freeze-drying and gold-spraying, the distribution and morphology of microorganisms on the surface of biological sponge iron and biological ceramsite were observed by SEM.

The surface of biological sponge iron and biological ceramsite fillers change obviously. The rough and porous surface is almost covered by microorganisms and their metabolites and becomes rougher as shown in Figure 4. A large number of small bacterial micelles with a diameter of $0.5\ \mu\text{m}$ – $1\ \mu\text{m}$ are attached to the surface of biological sponge iron. It can be seen from Figure 4(a) that small bacterial micelles are interconnected, and the extracellular polymers produced by the bacteria form large micelles through bonding action, which bond the individual microorganisms. The surface of biological ceramsite forms the visible rod-shaped bacteria as shown in Figure 4(b). The surfaces of biological fillers have $0.5\ \mu\text{m}$ – $2\ \mu\text{m}$ holes for organic nutrients and gas in and out.

3.3. COD Removal. It can be ascertained from Figure 5 that the average COD concentration of raw water is 232.90 mg/L. The COD concentrations of #1, #2, #3, #4, and #5 reactors in effluent are approximately 40 mg/L, which is significantly better than the Ctrl group without any filler (the average COD concentration in effluent is 161.75 mg/L). COD removal efficiency shows that #1 > #2 > #3 > #4 > #5, with average removal rates of 87.77%, 83.61%, 80.26%, 79.98%, and 69.91%, respectively, and the variances of COD removal rates of #1, #2, #3, #4, and #5 are 0.0012, 0.0179, 0.0076, 0.0080, and 0.0212, respectively. The removal efficiency of pure sponge iron and pure ceramsite is slightly better, because in neutral or slightly acidic environment, the new ecology [H] and Fe^{2+} generated by electrode reaction can have REDOX reaction with many components in wastewater, reduce COD concentration, and improve biodegradability [23]. Therefore, organic pollutants have been better removed.

3.4. TP Removal. Figure 6 shows that the average TP concentration of raw water is 15.19 mg/L, and the average TP concentrations of Ctrl, #1, #2, #3, #4, and #5 reactors in effluent are 11.57 mg/L, 0.38 mg/L, 1.29 mg/L, 1.32 mg/L, 1.55 mg/L, and 1.77 mg/L, respectively. The TP removal efficiency in each reactor is good and stable. However, the pure sponge iron has the best TP removal efficiency, with a removal rate of 97.2%, because the Fe ions (Fe^{2+} and Fe^{3+}) dissolved by biological sponge iron have strong flocculation and precipitation effect on phosphorus and can achieve sustained and stable phosphorus removal efficiency. Thus, the TP removal rate of sponge iron is as high as 97.2%. The TP removal rates of #2, #3, #4, and #5 reactors are 90.7%, 90.4%, 88.7%, and 87.2%, respectively, and the variances of TP removal rates of #1, #2, #3, #4, and #5 are 0.0002, 0.0021, 0.0030, 0.0121, and 0.0063, respectively.

The negative TP removal rate of the Ctrl group is due to the fact that the number of microorganisms in the raw water was scarce, so the microorganisms cannot be enriched and retained, and the degradation effect of the microorganisms is minimal. On the other hand, the TP removal is mainly dependent on adsorption and degradation. Because there is no filler in the Ctrl group, the phosphorus cannot be removed but deposited. The TP concentration in effluent is higher than that in influent and the curves of the Ctrl group and the raw water almost coincide in the later stage.

3.5. N Removal

3.5.1. $\text{NH}_3\text{-N}$ Removal. Figure 7 shows that the $\text{NH}_3\text{-N}$ removal rates of Ctrl, #1, #2, #3, #4, and #5 reactors are 48.15%, 71.17%, 85.29%, 75.68%, 75.99%, and 68.00%, respectively. The $\text{NH}_3\text{-N}$ removal efficiency of pure ceramsite is the best. The device is in a continuous aeration state, so that the $\text{NH}_3\text{-N}$ in sewage can be fully aerobic nitrification reaction. The aerobic nitrification process is carried out in two steps: firstly, $\text{NH}_3\text{-N}$ is oxidized to nitrite nitrogen ($\text{NO}_2\text{-N}$) by aerobic ammonia-oxidizing bacteria, and then $\text{NO}_2\text{-N}$ is oxidized to nitrate nitrogen ($\text{NO}_3\text{-N}$) under the action of nitrite-oxidizing bacteria [24, 25]. With the growth

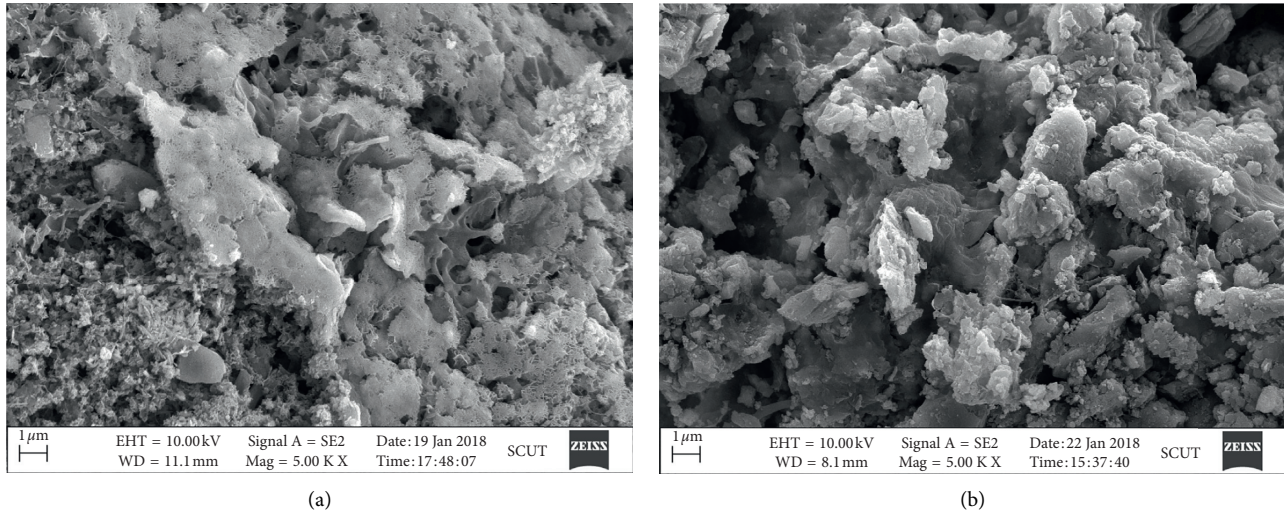


FIGURE 4: Electron microscopy images, (a) biological sponge iron and (b) biological ceramsite.

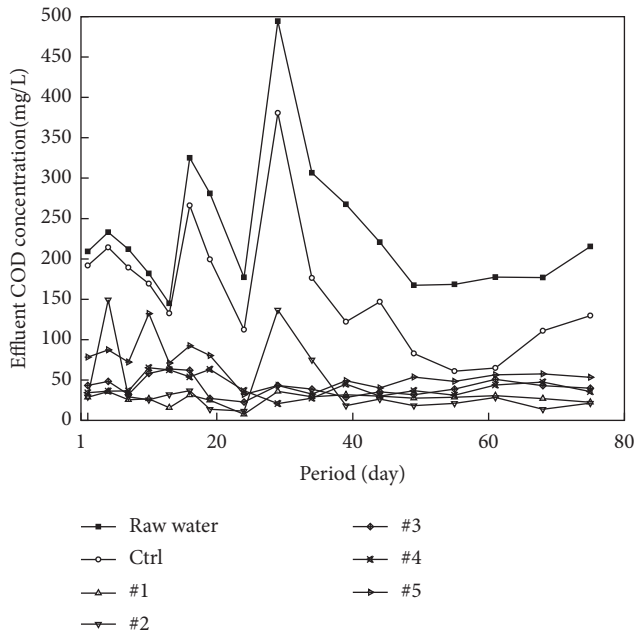


FIGURE 5: Effluent COD concentration of each group.

and metabolism of microorganisms in the reactor, the $\text{NH}_3\text{-N}$ concentration gradually decreases due to cell synthesis and nitrification. Thus, $\text{NH}_3\text{-N}$ removal is completed in the reactor.

3.5.2. TN Removal. The TN removal efficiencies of #1, #3, #4, and #5 reactors are relatively stable and good, with average removal rates of 68.03%, 70.60%, 70.21%, and 65.04%, respectively. However, the effluent TN concentration of raw water, Ctrl, and #2 reactors is significantly higher as shown in Figure 8. Although the $\text{NH}_3\text{-N}$ removal rate in #2 reactor is high and the nitrification reaction is sufficient, the content of nitrate generated is high and the N removal is

not completed, resulting in the high TN concentration, and the removal rate is only 48.16%.

It can be seen from the above that the removal efficiencies of COD, TP, $\text{NH}_3\text{-N}$, and TN in the reactors with sponge iron are all good. On the one hand, from the XRD of fresh sponge iron, it is concluded that the presence of Fe_3O_4 , Fe_2O_3 , Fe_3C , and Fe_2CO_3 determines the strong reducing property of sponge iron and provides reducing electrons for efficient denitrification. As a chemical catalyst, Fe ions speed up the transport of nutrients by increasing the permeability of nitrifying bacterial cell membrane, increasing the reaction rate. On the other hand, biochemical reactions will produce organic acids and CO_2 , resulting in the reduction of pH in the reactor [26], which is conducive to the reduction of nitrate to generate gaseous nitrogen, thus improving the TN removal efficiency in the reactors of sponge iron.

3.6. Abundance and Diversity of Species on Fillers Surface

3.6.1. Relative Abundance of Species. Figure 9 shows the relative abundance distribution of species under phylum level in reactors [27]. It shows species with relative abundance greater than or equal to 1%, while the relative abundance is less than 1%; unclassified and unidentified are classified as others. It can be seen from Figure 9 that species produced during sewage purification mainly include Planctomycetes, Firmicutes, Acidobacteria, Bacteroidetes, Proteobacteria, Actinobacteria, Chloroflexi, Nitrospirae, Verrucomicrobia, and OD1.

As can be seen from Figure 9, Ctrl, #1, #2, #3, #4, and #5 reactors are all dominated by Proteobacteria, accounting for 35.74%, 59.79%, 53.02%, 51.14%, 83.20%, and 69.33%, respectively. Bacteroidetes accounted for 36.02%, 22.15%, 7.64%, and 20.50% in Ctrl, #2, #4, and #5 reactors, respectively, and Firmicutes accounted for 14.91% and 45.46% in #1 and #3 reactors, respectively. In #2 reactor of the 6 groups, Acidobacteria, OD1, Chloroflexi, Planctomycetes, and Nitrospirae are all the highest, accounting for 4.53%,

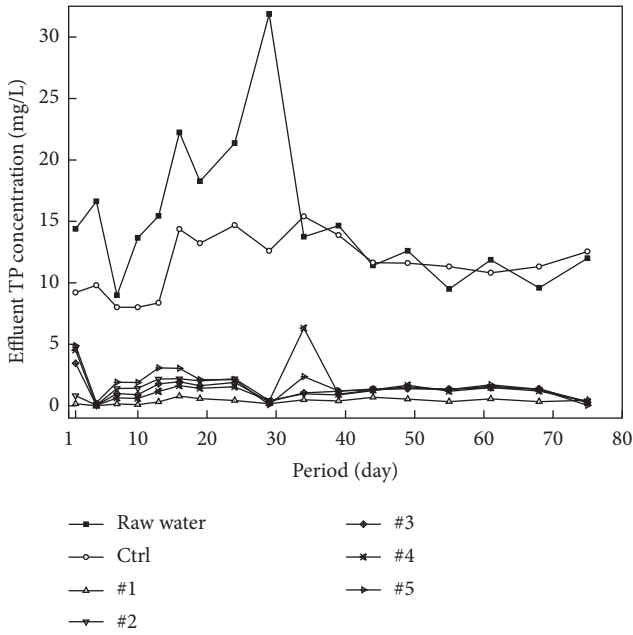


FIGURE 6: Effluent TP concentration of each group.

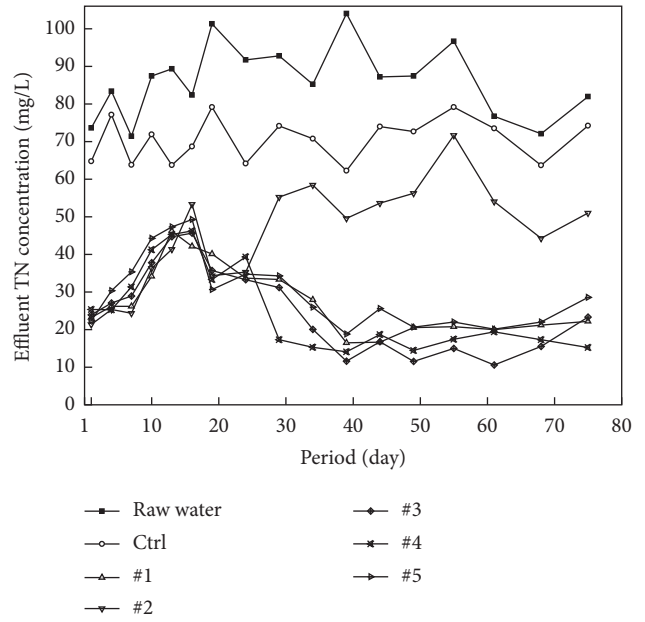


FIGURE 8: Effluent TN concentration of each group.

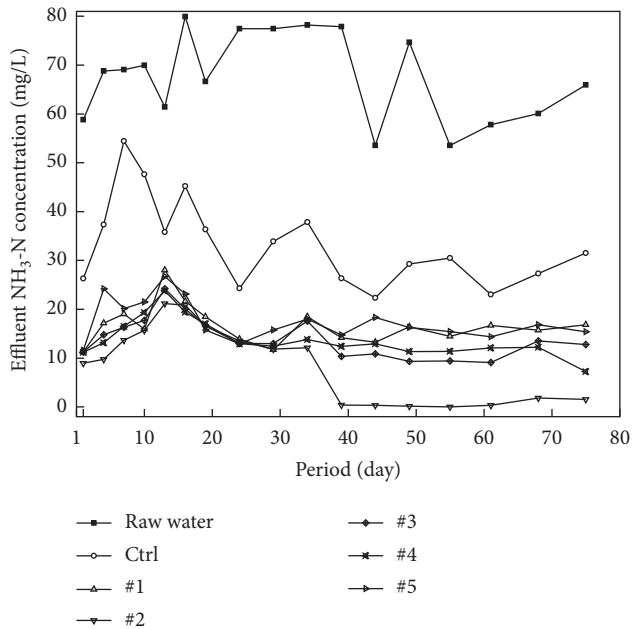


FIGURE 7: Effluent NH₃-N concentration of each group.

1.35%, 2.59%, 6.42%, and 4.59%, respectively. In #1 reactor of the 6 groups, Actinobacteria is the highest, accounting for 12.34%, Verrucomicrobia is the lowest, accounting for 0.06%, and there is no Nitrospirae. Figure 10 shows species abundance clustering heatmap under phylum level. The relative abundances of species under phylum level in #3 and #4 reactors are similar, and the relative abundances of species of #5 are the highest except for Actinobacteria, Firmicutes, and Proteobacteria in #3, #4, and #5 reactors.

Proteobacteria are Gram-negative bacteria, and their species diversity and genetic diversity are extremely

abundant, which determines that it is widely found in various environments, representing the largest group in the whole bacterial domain [28].

3.6.2. *Community Diversity.* The OTU in the sample was arranged according to the relative abundance from large to small to obtain the corresponding sequence number, and then the sequence number of the OTU was taken as the *x*-coordinate. For example, “200” represents the OTU ranked 200th in terms of abundance in the sample. The *y*-coordinate represents the relative percentage (take log) of the sequence number in the OTU of this rank [29]. These points were connected with polylines to draw the rank-abundance curve, as shown in Figure 11.

The rank-abundance curves reflect intuitively the abundance and regularity of the species. Abundance can be determined by the length of the curve on the *x*-coordinate; the longer the line, the more abundant the species composition. According to the curve trend, the uniformity of species composition can be seen. The smoother and lower the line is, the higher the uniformity of species composition will be. However, if the line is straight down, the dominant bacteria group in the sample takes up a large proportion and the diversity will be low.

The number of species in Ctrl reactor is 757, and the number of species in #1, #2, #3, #4, and #5 reactors is 563, 762, 278, 403, and 705, respectively. Species are the most abundant in #2 reactor. However, there is no significant difference in the smoothness among the samples, indicating that the uniformity of the species composition is similar. Observed from left to right on the *x*-coordinate, the relative abundance in #3 reactor plummets from the highest point of 0.42214 to 0.00706, the relative abundance in #4 reactor drops sharply from 0.26345 to 0.00944, and the relative abundance in Ctrl and #2 reactors drops smoothly from

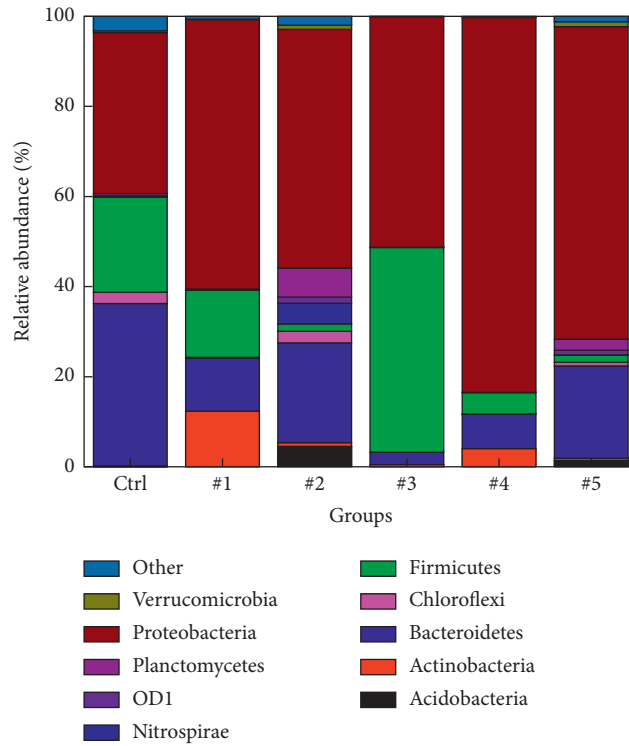


FIGURE 9: Relative abundance distributions of species under phylum level in reactors.

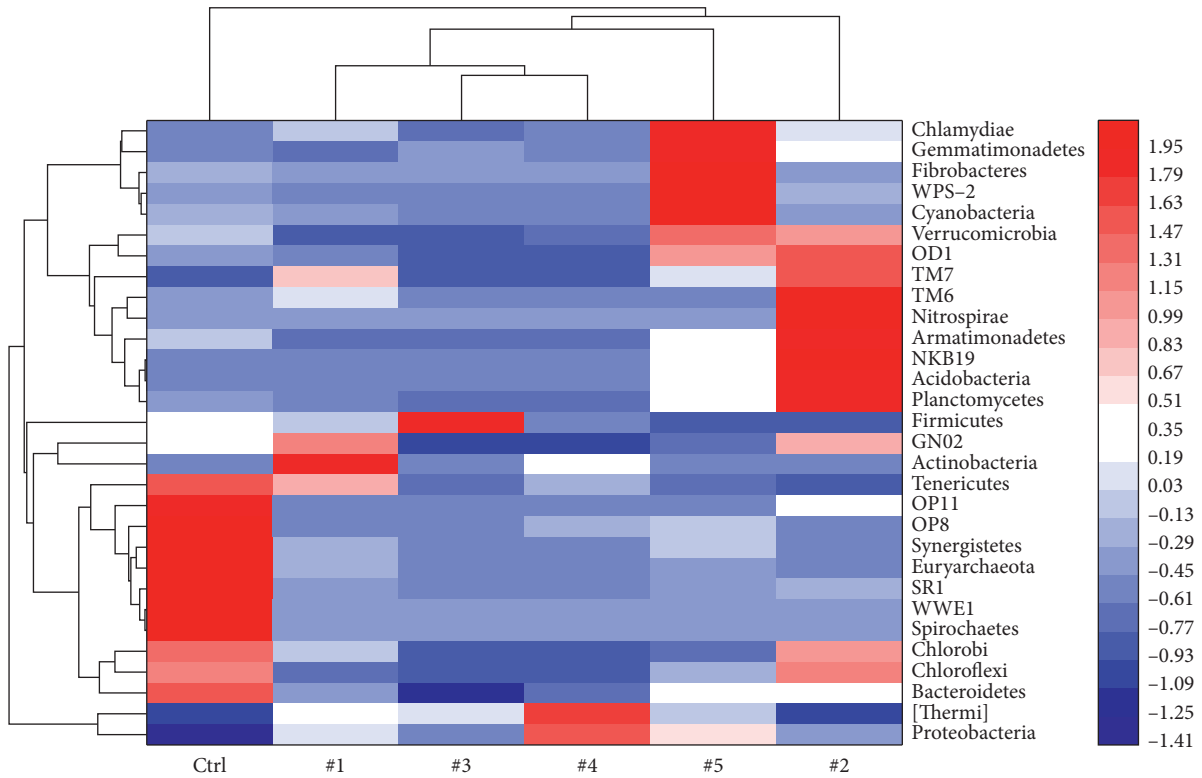


FIGURE 10: Species abundance clustering heatmap under phylum level.

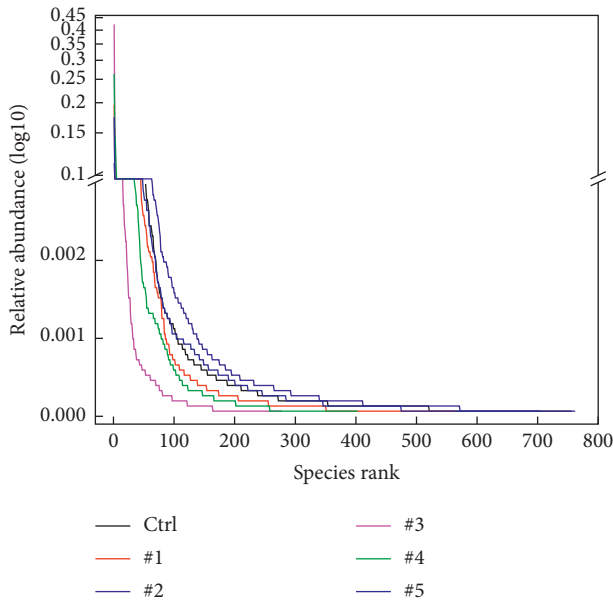


FIGURE 11: Rank-abundance curves of species.

0.07096 and 0.11215 to 0.02317 and 0.02475, respectively. The results showed that the dominant bacteria groups in #3 and #4 reactors have a high proportion and low diversity, while the species diversity in Ctrl and #2 reactors was high.

Compared with the Ctrl group, the abundance and diversity of species are decreased in #1, #3, #4, and #5 reactors and increased in #2 reactor. The order of abundance and diversity is #2 > Ctrl > #5 > #1 > #4 > #3. The results showed that ceramsite filler can improve the abundance and diversity of microorganisms in the reactors, and the higher the content of ceramsite in the reactors with ceramsite filler is, the higher the abundance and diversity will be, and the sponge filler and ceramsite filler can be mixed for the purification of urban sewage river.

4. Conclusion

In this paper, the mixture of sponge iron ceramsite was used to purify the urban sewage river through the self-designed BAF, and the purification efficiency of the mixed fillers on the urban sewage river was analyzed by taking the removal effect and abundance and diversity of species as the observation indexes. The following detailed conclusions are drawn:

- (1) The microporous structure of sponge iron and ceramsite mixed fillers is suitable for microbial growth and they are ideal fillers for biological sewage treatment technology. The presence of Fe_3O_4 , Fe_2O_3 , Fe_3C , and Fe_2CO_3 in sponge iron determines that sponge iron has strong reducibility and provides electrons for efficient denitrification. $\text{NaAlSi}_3\text{O}_8$ in ceramsite filler plays a significant role in phosphorus adsorption.
- (2) The COD removal rate and TP removal rate are all the highest in #1 reactor and the variances of COD

removal rate and TP removal rate are all the lowest in #1 reactor. The COD removal rates of mixed fillers in #3, #4, and #5 reactors are 7.51%, 7.79%, and 17.86% lower than sponge iron in #1 reactor, respectively. The TP removal rates of mixed fillers in #3, #4, and #5 reactors are 6.8%, 8.5%, and 10.0% lower than sponge iron in #1 reactor, respectively, and the $\text{NH}_3\text{-N}$ and TN removal efficiencies of mixed fillers are good. The mixture of ceramsite and sponge iron can hinder the hardening of sponge iron and ensures the removal efficiency of fillers.

- (3) The ceramsite filler can improve the abundance and diversity of microorganisms in the reactors; the higher the content of ceramsite in the reactors with ceramsite filler is, the higher the abundance and diversity will be; and the sponge filler and ceramsite filler can be mixed for the purification of urban sewage river.

Data Availability

The data used to support the findings of this study are available from the corresponding author upon request.

Conflicts of Interest

The authors declare that they have no conflicts of interest regarding the publication of this paper.

Acknowledgments

This study was financially supported by the Science and Technology Major Project for the Control and Management of Water Pollution in China (2015ZX07204-002) and the Natural Science Foundation of Guangdong Province, China (2016A030313021).

References

- [1] Y. Liu, B. D. Wang, Q. J. Zhang, C. Cui, and X. Deng, "Research on water resources reusing in northwest China," *Ground Water*, vol. 33, no. 4, pp. 107–110, 2011, in Chinese.
- [2] X. Cai, L. Yao, Y. Hu et al., "Particle-attached microorganism oxidation of ammonia in a hypereutrophic urban river," *Journal of Basic Microbiology*, vol. 59, no. 5, pp. 511–524, 2019.
- [3] A. D. Sutadian, N. Muttill, A. G. Yilmaz, and B. J. C. Perera, "Development of river water quality indices—a review," *Environmental Monitoring and Assessment*, vol. 188, no. 1, 2015.
- [4] S. Tiwari, R. Babbar, and G. Kaur, "Performance evaluation of two ANFIS models for predicting water quality index of river Satluj (India)," *Advances in Civil Engineering*, vol. 2018, no. 4, 10 pages, Article ID 8971079, 2018.
- [5] L. J. Gao, "Comparison of biological aerated filtration performance between zeolite media and ceramsite media," *Technology of Water Treatment*, vol. 35, no. 12, pp. 53–57, 2009, in Chinese.
- [6] H. F. Zhang, Y. J. Liu, and Z. Z. Zeng, "Study of biological aerated filter for sauce wastewater advanced treatment with spongy iron and argil granule," *Journal of Anhui Agricultural Sciences*, vol. 39, no. 326, pp. 597–599, 2011, in Chinese.

- [7] X. X. Zhang, L. J. Qin, C. C. Huang, T. T. Kong, X. J. Bai, and Y. B. Liu, "Study on the selection of immobilized carrier and its performance," *Chemical Industry and Engineering Progress*, vol. 30, no. 243, pp. 212–217, 2011, in Chinese.
- [8] J. Li, J. Li, and Y. Li, "Cadmium removal from wastewater by sponge iron sphere prepared by charcoal direct reduction," *Journal of Environmental Sciences*, vol. 21, no. s1, pp. s60–s64, 2009.
- [9] G. Z. Zhang, Q. Liao, and Y. Z. Wang, "Research progress in immobilized microorganisms carrier material," *Materials Review*, vol. 25, pp. 109–113, 2011, in Chinese.
- [10] C. Wen, X. Xu, Y. Fan, C. Xiao, and C. Ma, "Pretreatment of water-based seed coating wastewater by combined coagulation and sponge-iron-catalyzed ozonation technology," *Chemosphere*, vol. 206, no. 9, pp. 238–247, 2018.
- [11] J. Li, W. X. Li, Z. Y. Wei, Y. Li, and X. Wang, "Mechanism of cooperative phosphorus removal by sponge iron and microorganisms," *China Water & Wastewater*, vol. 29, no. 355, pp. 134–137, 2013, in Chinese.
- [12] M. Wang, J. C. Li, Y. Mao et al., "Decolorization of dye wastewater with spongy-iron induction-heating fixed bed reactor," *China Environmental Science*, vol. 34, pp. 67–74, 2014, in Chinese.
- [13] S. Y. Chang, T. Wu, and J. J. Zhao, "Effect of planting different submerged macrophytes groups on water purification of beidagang reservoir," *Chinese Journal of Environmental Engineering*, vol. 10, pp. 443–448, 2016, in Chinese.
- [14] H. S. Lee, S. J. Park, and T. I. Yoon, "Wastewater treatment in a hybrid biological reactor using powdered minerals: effects of organic loading rates on COD removal and nitrification," *Process Biochemistry*, vol. 38, no. 1, pp. 81–88, 2002.
- [15] Q. Wan, Y. Wu, X. Wang et al., "Study on the characteristics of the micro-pollution river purified by the immobilized carrier filler sponge iron," *Chemical Industry and Engineering Progress*, vol. 37, no. 5, pp. 1999–2009, 2018, in Chinese.
- [16] Y. Wu, "Experimental study based on sponge iron/ceramsite mixed fillers synergize elcon algae to purify polluted river water," Dissertation, Xi'an University of Science and Technology, Xi'an, China, 2017.
- [17] P. Fongsatitkul, D. G. Wareham, and P. Elefsiniotis, "Treatment of four industrial wastewaters by sequencing batch reactors: evaluation of COD, TKN and TP removal," *Environmental Technology*, vol. 29, no. 11, pp. 1257–1264, 2018.
- [18] R. Roseth, "Shell sand: a new filter medium for constructed wetlands and wastewater treatment," *Journal of Environmental Science and Health*, vol. 35, no. 8, pp. 1335–1355, 2008.
- [19] Y. Xie, X. L. Zhou, and Q. W. Li, "Treatment of municipal wastewater using self-made fly ash ceramsite as filler of BAF," *Journal of Material Science & Engineering*, vol. 35, no. 166, pp. 154–162, 2017, in Chinese.
- [20] Y. Y. Zheng, Y. F. Yu, Y. Li, C. S. Wu, W. W. Liu, and C. Q. Liu, "Adsorption of phosphorus or ammonia nitrogen by ceramsite made from waterworks sludge," *Chinese Journal of Environmental Engineering*, vol. 9, pp. 261–267, 2015, in Chinese.
- [21] L. Ding and P. Wang, "Study progress of using sponge iron in water treatment process and the existing problems," *China Water & Wastewater*, vol. 20, no. 3, pp. 30–32, 2004, in Chinese.
- [22] L. F. Chen, J. Q. Lin, D. Pan et al., "Ammonium removal by a newly isolated heterotrophic nitrification–aerobic denitrification bacteria *Pseudomonas stutzeri* SDU10 and its potential in treatment of piggery wastewater," *Current Microbiology*, vol. 77, no. 6, pp. 2792–2801, 2020.
- [23] D. Hira, N. Aiko, Y. Yabuki, and T. Fujii, "Impact of aerobic acclimation on the nitrification performance and microbial community of landfill leachate sludge," *Journal of Environmental Management*, vol. 209, no. 1, pp. 188–194, 2018.
- [24] J. Wang, B. Gong, Y. Wang, Y. Wen, J. Zhou, and Q. He, "The potential multiple mechanisms and microbial communities in simultaneous nitrification and denitrification process treating high carbon and nitrogen concentration saline wastewater," *Bioresource Technology*, vol. 243, no. 11, pp. 708–715, 2017.
- [25] S. Y. Lu, Z. F. Wan, F. M. Li, and X. Q. Zhang, "Ammonia nitrogen adsorption and desorption characteristics of twenty-nine kinds of constructed wetland substrates," *Research of Environmental Sciences*, vol. 29, no. 223, pp. 91–98, 2016, in Chinese.
- [26] N. Ma, Y. E. Wang, J. Li, and Y. M. Zhang, "Application of new water treatment material sponge iron in wastewater treatment," *Environmental Science and Management*, vol. 39, no. 201, pp. 75–77, 2014, in Chinese.
- [27] Y. X. Xie, A. J. Wan, H. J. Dong, X. M. Wang, and Y. P. Wu, "An iron-carbon-activated carbon and zeolite composite filter, anaerobic-aerobic integrated denitrification device for nitrogen removal in low C/N ratio sewage," *Water Science & Technology*, vol. 261, no. 6, pp. 82–89, 2019.
- [28] I. Vaz-Moreira, O. C. Nunes, and C. M. Manaia, "Ubiquitous and persistent Proteobacteria and other Gram-negative bacteria in drinking water," *Science of the Total Environment*, vol. 586, no. 15, pp. 1141–1149, 2017.
- [29] Z. Q. Song, L. Wang, X. H. Liu, and F. Liang, "Diversities of Firmicutes in four hot springs in yunnan and tibet," *Bio-technology*, vol. 25, no. 150, pp. 32–82, 2015, in Chinese.